The effect of measurement errors on the performance of the Exponentially Weighted Moving Average control charts for the Ratio of Two Normally Distributed Variables

H D Nguyen, Kim Phuc Tran, K.D Tran

The effect of measurement errors on the performance of the Exponentially Weighted Moving Average control charts for the Ratio of Two Normally Distributed Variables

H. D. Nguyen[a,b], K. P. Tran[b], K.D. Tran[c]

[a] *Institute of Artificial Intelligence and Data Science, Dong A University, Danang, Vietnam*
[b] *GEMTEX Laboratory, Ecole Nationale Supérieure des Arts et Industries Textiles, Roubaix, France.*
[c] *Institute of Research and Development, Duy Tan University, Danang 550000, Vietnam*

Abstract

Investigating the effect of measurement errors on the control chart monitoring the ratio of two normal random variables is an important task to facilitate the use of this kind of control chart in practice. Moreover, a deep insight into the problem can help practitioners to find a way to reduce unexpected impacts of measurement errors on the chart performance. This paper provides a study on the performance of the exponentially weighted moving average control chart monitoring the ratio in the presence of measurement errors. We extend the linear covariate error model applied in previous studies to a more general situation, which makes the study more realistic. The numerical results show that although the precision error and the accuracy error have negative influences on the proposed chart performance when these errors are not large these influences are not significant.

Keywords: Quality control, EWMA, Ratio distribution, Markov Chain, Measurement error.

1. Introduction

Statistical Process Control (SPC) refers to a standard methodology of quality control for monitoring and controlling a process based on tatistical methods. The main purpose of SPC is to ensure the efficient operation of the process.

*Corresponding author
Email address: kim-phuc.tran@ensait.fr (K. P. Tran)

SPC consists of many tools in which control charts are widely used to detect assignable causes that lead to changes in the process output. There are a large number of studies related to developing control charts with high performance that make their applications more efficient in the manufacturing process, see, for example, Bersimis et al. [1], Tran et al. [21], Teoh et al. [20] and Marcondes & Valk [11].

It has been demonstrated in the SPC literature that the ratio of two normal variables is a major concern in several studies. The motivation for these studies comes from the fact that this ratio is an essential characteristic to ensure the quality of products in many processes. For example, in the food industry, keeping the relative weights of two main ingredients could be a requirement to make sure the quality of a food recipe. In the pharmaceutical industry, the safety and the effectiveness of drugs could be guaranteed by stabilizing the proportion of two active ingredients. An overview of typical situations that require monitoring the ratio of two quantities has been discussed in Celano & Castagliola [4]. Concerning the methods of monitoring the ratio of two normal variables, several control charts have been suggested, see Celano et al. [5], Celano & Castagliola [4], and Tran et al. [21] for more details.

In practice, measurement error almost exists in all processes, ignoring the presence of the measurement error in designing control charts may lead to a misunderstanding about the statistical properties of the designed control charts. Recent studies related to this problem can be seen in Tran et al. [22],Khurshid & Chakraborty [9], Sabahno et al. [17], Hassani et al. [8], Daryabari et al. [7], Song et al. [18, 19] and Sabahno et al. [16]. For the case of control charts monitoring the ratio, Tran et al. [22] used a quite strict assumption that $z_1^* = \tau * z_0^*$ where z_1^* and z_0^* are the out-of-control ratios, respectively and the in-control ratio in the presence of measurement error and τ is the shift size. This assumption is not really reasonable in practice. Nguyen & Tran [13] extended this study by easing this assumption to make it more realistic. The authors provided an exact change of the process parameters from an in-control condition to an out-of-control status under the presence of measurement errors.

The use of the Exponentially Weighted Moving Average (EWMA) control chart has become increasingly popular in SPC literature. One of the reasons for the wide use of this type of chart is because it has "memory": it monitors a process based on the information from the whole process rather than the information from only the current condition. As a result, it is often more effective than several others in detecting process shifts. Recently, the EWMA control charts for monitoring the ratio of two normal variables (denoted by EWMA-RZ control chart) are proposed by Tran et al. [21]. The goal of this paper is to investigate the effect of measurement errors on the performance of EWMA-RZ control charts. In this paper, we aim to develop a new measurement error model to fully describe the impact of measurement errors on the EWMA-RZ control chart, an advanced chart that is very effective in detecting small shifts from a process. Instead of assuming an identity matrix in the linear covariate model, we consider a more general situation with a diagonal matrix. The motivation of the paper is (1) to ease the strict assumption about the relation between the out-of-control ratio and the in-control ratio in Tran et al. [22] as well as to extend the assumption of identity matrix in the linear covariate model applied in Nguyen & Tran [13], and (2) to investigate the impact of measurement errors on the EWMA-RZ control chart, and then to propose the ways to reduce the impact of measurement errors on the performance of this control chart when applied in practice. These improvements allow this study to overcome the disadvantages in previous studies on the control charts monitoring the ratio in the presence of measurement error and make it more efficient and realistic that could be useful for practitioners.

The paper is organized as follows. Section 2 presents a linear covariate error model for the ratio and an establishment of the change of the chart parameters and the model parameters from in-control condition to out-of-control status. The implementation and the design of the EWMA-RZ control chart with measurement errors are discussed in section 3 and section 4, respectively. The effect of measurement error on the EWMA-RZ control chart performance is presented in section 5. Section 6 is for an illustrative example of the implementation

of the EWMA-RZ control chart in the presence of measurement errors. Some concluding remarks are given in section 7.

2. Linear covariate error model for the sample of the ratio

In this section, we present a linear covariate error model for the sample ratio. A brief review of the distribution of the sample of the ratio can be seen in the Appendix. In Tran et al. [22], the authors supposed that the relation between the out-of-control ratio and the in-control ratio is independent of measurement errors (see equation (36) in Tran et al. [22] and the corresponding explanation). In practice, measurement errors may affect the true observations of the ratio. As a result, this relation should change with measurement errors. We will model accurately the change of parameters of a process after being shifted under the presence of measurement errors to see more clearly this variation.

Let us assume that, at time $i = 1, 2, \ldots$, a set of n consecutive items $\{\mathbf{W}_{i,1}, \mathbf{W}_{i,2}, ..., \mathbf{W}_{i,n}\}$ of the quality characteristic $\mathbf{W}$ is collected, where $\mathbf{W}_{i,j} = (X_{i,j}, Y_{i,j})^T \sim N(\boldsymbol{\mu}_{\mathbf{W}}, \boldsymbol{\Sigma}_{\mathbf{W}})$ is a bivariate normal vector with mean $\boldsymbol{\mu}_{\mathbf{W}}$ and variance-covariacne matrix $\boldsymbol{\Sigma}_{\mathbf{W}}$ defined as in (29). Due to measurement errors, the *true* quality characteristics $\mathbf{W}_{i,j}$ is unobservable. Instead, it is assessed from a set of $m \geq 1$ measurement operations, $\{\mathbf{W}^*_{i,j,1}, \mathbf{W}^*_{i,j,2}, ..., \mathbf{W}^*_{i,j,m}\}$. According to the linear covariate error model (Linna et al. [10]), we have

$$\mathbf{W}^*_{i,j,k} = \mathbf{A} + \mathbf{B}\mathbf{W}_{i,j} + \boldsymbol{\varepsilon}_{i,j,k}, k = 1, \ldots, m, \tag{1}$$

where $\mathbf{A}$ is a (2×1) vector of constants,

$$\mathbf{A} = \begin{pmatrix} a_X \\ a_Y \end{pmatrix}, \tag{2}$$

$\mathbf{B}$ is a (2×2) matrix, $\boldsymbol{\varepsilon} \sim N(\mathbf{0}, \boldsymbol{\Sigma}_M)$ is a centered bivariate normal random vector assumed to be independent of $\mathbf{W}$. The variance-covariance matrix in the distribution of $\boldsymbol{\varepsilon}$ is denoted by

$$\boldsymbol{\Sigma}_M = \begin{pmatrix} \sigma^2_{MX} & \rho_M \sigma_{MX} \sigma_{MY} \\ \rho_M \sigma_{MX} \sigma_{MY} & \sigma^2_{MY} \end{pmatrix}, \tag{3}$$

where σ_{MX} (resp. σ_{MY}) is the standard-deviation of measurement errors of X (resp. Y), and $\rho_M \in (-1, +1)$ is the corresponding coefficient of correlation.

In Linna et al. [10], the authors recommended an invertible $p \times p$ matrix of constants, often diagonal, for the matrix $\mathbf{B}$. Therefore, we assume that $\mathbf{B} = b\mathbf{I}_{2\times 2}$, where b is a constant, i.e.

$$\mathbf{B} = \begin{pmatrix} b & 0 \\ 0 & b \end{pmatrix}. \tag{4}$$

In paractice, the mean $\overline{\mathbf{W}}^*_{i,j} = (\bar{X}^*_{i,j}, \bar{Y}^*_{i,j})$ of the observable quantities $\{\mathbf{W}^*_{i,j,1}, \mathbf{W}^*_{i,j,2}, ..., \mathbf{W}^*_{i,j,m}\}$ is often considered as a represented value for the true value $\mathbf{W}_{i,j}$. This mean is calculated by

$$\begin{aligned} \overline{\mathbf{W}}^*_{i,j} &= \frac{1}{m}\sum_{k=1}^{m} \mathbf{W}^*_{i,j,k} \\ &= \frac{1}{m}\sum_{k=1}^{m} (\mathbf{A} + \mathbf{B}\mathbf{W}_{i,j} + \boldsymbol{\varepsilon}_{i,j,k}) \\ &= \mathbf{A} + \mathbf{B}\mathbf{W}_{i,j} + \frac{1}{m}\sum_{k=1}^{m} \boldsymbol{\varepsilon}_{i,j,k}. \end{aligned} \tag{5}$$

That is, $\overline{\mathbf{W}}^*_{i,j}$ is also a bivariate normal random vector with the mean vector and the variance-covariance matrix defined by

$$\boldsymbol{\mu}_{\mathbf{W}^*} = \mathbf{A} + \mathbf{B}\boldsymbol{\mu}_{\boldsymbol{W}}, \tag{6}$$

$$\boldsymbol{\Sigma}_{\mathbf{W}^*} = \mathbf{B}\boldsymbol{\Sigma}_{\boldsymbol{W}}\mathbf{B}^T + \frac{1}{m}\boldsymbol{\Sigma}_M = b^2\boldsymbol{\Sigma}_{\boldsymbol{W}} + \frac{1}{m}\boldsymbol{\Sigma}_M. \tag{7}$$

Let $\mu_{X^*}, \mu_{Y^*}, \sigma^2_{X^*}, \sigma^2_{Y^*}$ and ρ^* denote the mean, the variance and the coefficient of correlation of the two components $(\bar{X}^*_{i,j}, \bar{Y}^*_{i,j})$ of the vector $\overline{\mathbf{W}}^*_{i,j}$, respectively. Then, the equations (6) and (7) lead to

$$\mu_{X^*} = a_X + b\mu_X \tag{8}$$

$$\mu_{Y^*} = a_Y + b\mu_Y \tag{9}$$

$$\sigma^2_{X^*} = b^2\sigma^2_X + \frac{\sigma^2_{MX}}{m}, \tag{10}$$

$$\sigma^2_{Y^*} = b^2\sigma^2_Y + \frac{\sigma^2_{MY}}{m}, \tag{11}$$

$$\rho^* = \frac{b^2\rho\sigma_X\sigma_Y + \rho_M\frac{\sigma_{MX}\sigma_{MY}}{m}}{\sigma_{X^*}\sigma_{Y^*}}. \tag{12}$$

The equations (8)-(12) show a general change of $\mu_X, \mu_Y, \sigma^2_X, \sigma^2_Y$ and ρ under the presence of the measurement errors. In the sequel, we will represent these changes when the process is shifted from an in-control condition to an out-of-control status.

Let $\boldsymbol{\mu_{0,W}} = (\mu_{0,X}, \mu_{0,Y})^T$ and $\rho = \rho_0$ denote the mean vector and the coefficient of correlation between the two normal variables $X_{i,j}$ and $Y_{i,j}$ of when the process is in-control. The mean ratio is now $z_0 = \frac{\mu_{0,X}}{\mu_{0,Y}}$. Suppose that an abnormal condition shifts the in-control ratio z_0 to $z_1 = \tau z_0$, where τ is the shift size, and the in-control coefficient of correlation $\rho = \rho_0$ to $\rho = \rho_1$. In particular, we suppose that the in-control $\boldsymbol{\mu_{0,W}}$ is shifted to $\boldsymbol{\mu_{1,W}} = (\mu_{0,X} + \delta_X\sigma_X, \mu_{0,Y} + \delta_Y\sigma_Y)^T$ where δ_X and δ_Y represent the mean shift of $X_{i,j}$ and $Y_{i,j}$. Then, the equation $z_1 = \tau z_0$ becomes

$$\frac{\mu_{0,X} + \delta_X\sigma_X}{\mu_{0,Y} + \delta_Y\sigma_Y} = \tau \times \frac{\mu_{0,X}}{\mu_{0,Y}},$$

and we obtain the following formula:

$$1 + \delta_X\gamma_X = \tau(1 + \delta_Y\gamma_Y). \tag{13}$$

According to the equations (8)-(11), under the presence of measurement errors, the coefficients of variation $\gamma_{X^*} = \frac{\sigma_{X^*}}{\mu_{X^*}}$ and $\gamma_{Y^*} = \frac{\sigma_{Y^*}}{\mu_{Y^*}}$ of $\bar{X}^*_{i,j}$ and $\bar{Y}^*_{i,j}$ are equal to

$$\gamma_{X^*} = \frac{\sqrt{b^2\sigma_X^2 + \frac{\sigma_{MX}^2}{m}}}{a_X + b(\mu_{0,X} + \delta_X\sigma_X)}, \tag{14}$$

$$\gamma_{Y^*} = \frac{\sqrt{b^2\sigma_Y^2 + \frac{\sigma_{MY}^2}{m}}}{a_Y + b(\mu_{0,Y} + \delta_Y\sigma_Y)}. \tag{15}$$

Considering the fraction in (14), if we divide its numerator by σ_X, its denominator by $\mu_{0,X}$ and then use (13), the coefficient of variation γ_{X^*} can be rewritten by

$$\gamma_{X^*} = \frac{\sqrt{b^2 + \frac{\eta_X^2}{m}}}{b(1 + \delta_X\gamma_X) + \theta_X} \times \gamma_X = \frac{\sqrt{b^2 + \frac{\eta_X^2}{m}}}{b\tau(1 + \delta_Y\gamma_Y) + \theta_X} \times \gamma_X \tag{16}$$

where $\eta_X = \frac{\sigma_{MX}}{\sigma_X}$, $\theta_X = \frac{a_X}{\mu_{0,X}}$, and $\gamma_X = \frac{\sigma_X}{\mu_{0,X}}$.

In a similar way, the coefficients of variation γ_{Y^*} in (15), the coefficient of correlation ρ^* in (12) and the standard-deviation ratio $\omega^* = \frac{\sigma_{X^*}}{\sigma_{Y^*}}$ can be expressed

as

$$\gamma_{Y^*} = \frac{\sqrt{b^2+\frac{\eta_Y^2}{m}}}{b(1+\delta_Y\gamma_Y)+\theta_Y}\times\gamma_Y, \tag{17}$$

$$\rho^* = \frac{b^2\rho+\rho_M\frac{\eta_X\eta_Y}{m}}{\sqrt{b^2+\eta_X^2/m}\sqrt{b^2+\eta_Y^2/m}}, \tag{18}$$

$$\omega^* = \sqrt{\frac{b^2+\frac{\eta_X^2}{m}}{b^2+\frac{\eta_Y^2}{m}}}\times\omega, \tag{19}$$

where $\eta_Y=\frac{\sigma_{MY}}{\sigma_Y}$, $\theta_Y=\frac{a_Y}{\mu_{0,Y}}$, $\gamma_Y=\frac{\sigma_Y}{\mu_{0,Y}}$ and $\omega=\frac{\sigma_X}{\sigma_Y}$.

It should be considered that the in-control and out-of-control ratio under the presence of the measurement errors are

$$z_0^* = \frac{\mu_{0,X^*}}{\mu_{0,Y^*}}=\frac{b\mu_{0,X}+a_X}{b\mu_{0,Y}+a_Y}=\frac{b+\theta_X}{b+\theta_Y}\times z_0, \tag{20}$$

$$\begin{aligned} z_1^* &= \frac{\mu_{1,X^*}}{\mu_{1,Y^*}}=\frac{a_X+b(\mu_{0,X}+\delta_X\sigma_X)}{a_Y+b(\mu_{0,Y}+\delta_Y\sigma_Y)}=\frac{\theta_X+b(1+\delta_X\gamma_X)}{\theta_Y+(1+\delta_Y\gamma_Y)}\times z_0 \\ &= \frac{\theta_X+\tau(1+\delta_Y\gamma_Y)}{\theta_Y+(1+\delta_Y\gamma_Y)}\times z_0. \end{aligned} \tag{21}$$

Thus, in general we have $z_1^*\neq\tau z_0^*$.

3. Implementation of the EWMA-RZ control chart with measurement error

Consider a process with the same assumptions and notations as in the previous section. Supppose that the process is considered in-control as long as the ratio $Z=X/Y$ is still in an acceptable range. Similar to Tran et al. [22], after collecting the samples $\{\mathbf{W}_{i,j,1}^*,\mathbf{W}_{i,j,2}^*,...,\mathbf{W}_{i,j,m}^*\}$ at each sampling period $i=1,2,\ldots$, we suggest to monitor the statistic

$$\hat{Z}_i^*=\frac{\hat{\mu}_{X_i^*}}{\hat{\mu}_{Y_i^*}}=\frac{\bar{\bar{X}}_i^*}{\bar{\bar{Y}}_i^*}=\frac{\sum_{j=1}^n\bar{X}_{i,j}^*}{\sum_{j=1}^n\bar{Y}_{i,j}^*}, \tag{22}$$

where $\bar{\bar{X}}_i^*=\frac{1}{n}\sum_{j=1}^n\bar{X}_{i,j}^*$, $\bar{\bar{Y}}_i^*=\frac{1}{n}\sum_{j=1}^n\bar{Y}_{i,j}^*$, $\bar{X}_{i,j}^*$ and $\bar{Y}_{i,j}^*$ are two components of the bivariate normal vector $\overline{\mathbf{W}}_{i,j}^*$ in (5).

It can be seen from their definition that $\bar{\bar{X}}_i^*\sim N(\mu_{X^*},\frac{\sigma_{X^*}}{\sqrt{n}})$ and $\bar{\bar{Y}}^*\sim N(\mu_{Y^*},\frac{\sigma_{Y^*}}{\sqrt{n}})$. Therefore, the coefficients of variations $\gamma_{\bar{X}^*}$ and $\gamma_{\bar{Y}^*}$ of $\bar{X}_i^*$ and $\bar{Y}_i^*$, the standard-deviation ratio $\omega_{\hat{Z}^*}$ at each sampling period $i=1,2,\ldots$ are,

respectively, equal to

$$\gamma_{\bar{X}^*} = \frac{\sigma_{X^*}}{\mu_{X^*}\sqrt{n}} = \frac{\gamma_{X^*}}{\sqrt{n}}, \tag{23}$$

$$\gamma_{\bar{Y}^*} = \frac{\sigma_{Y^*}}{\mu_{Y^*}\sqrt{n}} = \frac{\gamma_{Y^*}}{\sqrt{n}}, \tag{24}$$

$$\omega_{\hat{Z}^*} = \frac{\sigma_{X^*}/\sqrt{n}}{\sigma_{Y^*}/\sqrt{n}} = \frac{\sigma_{X^*}}{\sigma_{Y^*}} = \omega^* \tag{25}$$

The *p.d.f* and the *c.d.f* of $\hat{Z}_i^*$ now can be obtained from (30) and (31) where γ_X, γ_Y, ω and ρ are replaced by $\gamma_{\bar{X}^*}$, $\gamma_{\bar{Y}^*}$, ω^* and ρ^* as defined in (23), (24), (25) and (18).

Since the distribution of $\hat{Z}_i^*$ is not symmetric, similar to Tran et al. [21], two one-sided charts to monitor $\hat{Z}_i^*$ will be considered. In the design of an one-sided EWMA control chart, the statistic $\hat{Z}_i^*$ is not monitored directly. Instead, the following statistic will be monitored:

- in an upward EWMA chart (denoted as "EWMA-RZ$^+$" in the remainder of the paper) that aims at detecting an increase in the ratio,

$$Y_i^{*+} = \max(z_0^*, (1-\lambda^+)Y_{i-1}^{*+} + \lambda^+ \hat{Z}_i^*) \tag{26}$$

  where $Y_0^{*+} = z_0^*$ is an initial value. The corresponding upper control limit is $UCL^+ = K^+ \times z_0^*$ ($K^+ > 1$), and by the construction the lower control limit is $LCL^+ = z_0^*$.

- in a downward EWMA chart (denoted as "EWMA-RZ$^-$" in the remainder of the paper) that aims at detecting a decrease in the ratio,

$$Y_i^{*-} = \min(z_0^*, (1-\lambda^-)Y_{i-1}^{*-} + \lambda^- \hat{Z}_i^*) \tag{27}$$

  where $Y_0^{*-} = z_0^*$ is an initial value. The corresponding lower control limit is $LCL^- = K^- \times z_0^*$ ($K^- < 1$), and by the construction, the upper control limit is $UCL^- = z_0^*$.

It should be considered that the control limits are considered in these forms rather than the general ones involving the mean and the standard deviation of Z_i because the distribution of $\hat{Z}_i^*$ has no moments. The two EWMA-RZ$^-$ and EWMA-RZ$^+$ charts above are defined when the smoothings $\lambda^+ \in (0, 1]$, $\lambda^- \in (0, 1]$ and the chart parameters K^+, K^- are defined.

4. Design of optimal EWMA-RZ Control Charts with measurement error

It is customary that the average run length (ARL) is used to measure the performance of a control chart. This measure counts the average number of samples before the chart signals an "out-of-control condition" after an occurrence of an assignable cause. When the process runs in-control, it is denoted by ARL_0; otherwise, it is denoted by ARL_1. In the Appendix, we present a method to compute this measure based on a discrete Markov chain approach proposed by Brook & Evans [2].

In practice, when an exact value of the shift size of τ is predicted at the design stage, the EWMA-RZ charts can be optimally designed in terms of ARL. However, it is not always the case since this size cannot be anticipated exactly. This may lead to the poor performance of the designed chart. Therefore, in this study, we suggest to optimally design the EWMA-RZ charts under the presence of the measurement errors in terms of expected average run length ($EARL$), which is defined as

$$EARL = \int_{\Omega} ARL \times f_{\tau}(\tau)\mathrm{d}\tau, \tag{28}$$

where $f_{\tau}(\tau)$ is a $p.d.f$ of the random shift size τ over a support Ω and ARL is defined as in (35). In the SPC literature, a uniform distribution has been proposed to τ over a prespecified interval $[a, b]$ (see, for example, Castagliola et al. [3], Celano et al. [6] and Tran et al. [21]). That is, $f_{\tau}(\tau) = \frac{1}{b-a}$ for $\tau \in \Omega = [a, b]$.

With respcet to this measure, the optimal design of the proposed charts consists of finding optimal couples (K^{*-}, λ^{*-}) or (K^{*+}, λ^{*+}) such that:

- for the EWMA-RZ$^-$ chart,

$$(K^{*-}, \lambda^{*-}) = \underset{(K^-, \lambda^-)}{\arg\min}\, EARL(n, K^-, \lambda^-, \rho_1, \gamma_{X^*}, \gamma_{Y^*}, \rho^*, \omega^*)$$

  subject to the constraint

$$ARL(n, K^-, \lambda^-, \gamma_{X^*}, \gamma_{Y^*}, \rho^*, \omega^*, \rho_1 = \rho_0, \tau = 1) = ARL_0,$$

- for the EWMA-RZ$^+$ chart:

$$(K^{*+}, \lambda^{*+}) = \underset{(K^+, \lambda^+)}{\arg\min}\, EARL(n, K^+, \lambda^+, \rho_1, \gamma_{X^*}, \gamma_{Y^*}, \rho^*, \omega^*)$$

subject to the constraint

$$ARL(n, K^+, \lambda^+, \gamma_{X^*}, \gamma_{Y^*}, \rho^*, \omega^*, \rho_1 = \rho_0, \tau = 1) = ARL_0.$$

5. The effect of measurement errors on the EWMA-RZ control charts

We investigate in this section the statistical performance of the EWMA-RZ control chart in the presence of measurement errors. Without loss of generality, we assume that $z_0 = 1$ and $\delta_Y = 1$. The in-control value ARL_0 is set at 200. We also suppose that the shift size τ follows a uniform distribution over the interval $\Omega_D = [0.9, 1)$ (EWMA-RZ$^-$ chart) and $\Omega_I = [1, 1.1)$ (EWMA-RZ$^+$ chart). The numerical results are rounded to 4 decimal places. The program for the numerical analysis in this paper is written on the ScicosLab 4.4.2 software which is available upon request from authors.

The optimal couples (K^{*-}, λ^{*-}) of the EWMA-RZ$^-$ chart and (K^{*+}, λ^{*+}) of the EWMA-RZ$^+$ chart for several situations of parameters, which are $\gamma_X \in \{0.01, 0.2\}$, $\gamma_Y \in \{0.01, 0.2\}$, $n \in \{1, 5, 7, 10, 15\}$, $\rho_0 \in \{-0.8, -0.4, 0, 0.4, 0.8\}$, $m = 1, b = 1$, and given $\theta_X = \theta_Y = 0.01$, $\eta_X = \eta_Y = 0.28$, $\rho_M = 0.5$ are presented in Table 1. Since the in-control ratio z_0 is set at $z_0 = 1$, the value of $K^{*-}(K^{*+})$ is also the value of the corresponding $LCL^-(UCL^+)$. The reason for these specific values of parameters was discussed further in Tran et al. [22]. The other values of these optimal couples for other cases of parameters are not presented here but are available upon request from authors.

It can be seen from the Table 1 that the optimal value $\lambda^{*-}(\lambda^{*+})$ depends on the parameters γ_X, γ_Y, n and ρ_0. For example, given the value of (γ_X, γ_Y), when n and/or ρ_0 increase, $\lambda^{*-}(\lambda^{*+})$ increases. Take the case $\gamma_X = \gamma_Y = 0.01$ as an example, we have $\lambda^{*-} = 0.1964$ for $n = 1, \rho_0 = -0.8$ and $\lambda^{*-} = 0.9952$ for $n = 15, \rho_0 = 0.4$. Similarly, the optimal chart parameter $K^{*-}(K^{*+})$, and then the control limit, also change with these parameters. Given the value of n, ρ_0, when (γ_X, γ_Y) increases, K^{*-} decreases while K^{*+} increases. For example, with $n = 5, \rho_0 = 0.0$, we have $K^{*-} = 0.9910$, $K^{*+} = 0.4558$ when $(\gamma_X, \gamma_Y) = (0.01, 0.01)$ and $K^{*-} = 0.9651$, $K^{*+} = 0.0545$ when $(\gamma_X, \gamma_Y) = (0.2, 0.2)$. Moreover, in this table, in the first part ($\gamma_X = 0.01$), the optimal value for λ is very close to 1, especially for $\gamma_0 = 0.8$. This is the case of Shewhart RZ chart, which is preferable (in terms of simplicity) than the EWMA

Table 1: Optimal couples (K^{*-}, λ^{*-}) (first row) and (K^{*+}, λ^{*+}) (second row) for the EWMA-RZ control chart in the presence of Measurement Error, for $z_0 = 1$, $ARL_0 = 200$, $m = 1, b = 1$, $\theta_X = \theta_Y = 0.01$, $\eta_X = \eta_Y = 0.28$, $\rho_M = 0.5$, $n \in \{1, 5, 7, 10, 15\}$, $\gamma_X \in \{0.01, 0.2\}$, $\gamma_Y \in \{0.01, 0.2\}$ and $\rho_0 \in \{-0.8, -0.4, 0, 0.4, 0.8\}$

γ_X	γ_Y	ρ_0	$n = 1$	$n = 5$	$n = 7$	$n = 10$	$n = 15$
0.01	0.01	−0.8	(0.9847, 0.1946)	(0.9897, 0.3664)	(0.9905, 0.4151)	(0.9912, 0.4858)	(0.9920, 0.5671)
			(1.0152, 0.1813)	(1.0102, 0.3518)	(1.0095, 0.4074)	(1.0087, 0.4650)	(1.0080, 0.5568)
		−0.4	(0.9857, 0.2119)	(0.9904, 0.3980)	(0.9910, 0.4582)	(0.9916, 0.5390)	(0.9923, 0.6360)
			(1.0143, 0.2013)	(1.0097, 0.3899)	(1.0091, 0.4558)	(1.0083, 0.5246)	(1.0076, 0.6203)
		0.0	(0.9868, 0.2395)	(0.9910, 0.4558)	(0.9916, 0.5304)	(0.9921, 0.6203)	(0.9925, 0.7646)
			(1.0132, 0.2302)	(1.0090, 0.4475)	(1.0083, 0.5139)	(1.0078, 0.6063)	(1.0075, 0.7501)
		0.4	(0.9883, 0.2912)	(0.9919, 0.5595)	(0.9923, 0.6517)	(0.9925, 0.8049)	(0.9927, 0.9952)
			(1.0116, 0.2763)	(1.0082, 0.5578)	(1.0077, 0.6496)	(1.0075, 0.7863)	(1.0073, 0.9807)
		0.8	(0.9907, 0.4308)	(0.9926, 0.9405)	(0.9934, 0.9997)	(0.9945, 0.9995)	(0.9955, 0.9999)
			(1.0092, 0.4190)	(1.0074, 0.9357)	(1.0066, 0.9997)	(1.0055, 0.9995)	(1.0045, 0.9999)
0.20	0.20	−0.8	(0.9184, 0.0500)	(0.9578, 0.0500)	(0.9636, 0.0500)	(0.9690, 0.0500)	(0.9742, 0.0501)
			(1.1681, 0.0500)	(1.0575, 0.0500)	(1.0473, 0.0500)	(1.0386, 0.0500)	(1.0308, 0.0500)
		−0.4	(0.9253, 0.0500)	(0.9620, 0.0501)	(0.9673, 0.0500)	(0.9722, 0.0500)	(0.9764, 0.0518)
			(1.1422, 0.0500)	(1.0499, 0.0500)	(1.0412, 0.0500)	(1.0337, 0.0501)	(1.0282, 0.0534)
		0.0	(0.9196, 0.0654)	(0.9651, 0.0545)	(0.9718, 0.0501)	(0.9760, 0.0502)	(0.9776, 0.0598)
			(1.1147, 0.0500)	(1.0416, 0.0501)	(1.0343, 0.0500)	(1.0287, 0.0515)	(1.0252, 0.0587)
		0.4	(0.9453, 0.0500)	(0.9736, 0.0500)	(0.9768, 0.0520)	(0.9780, 0.0615)	(0.9792, 0.0754)
			(1.0844, 0.0500)	(1.0344, 0.0565)	(1.0274, 0.0529)	(1.0247, 0.0607)	(1.0220, 0.0706)
		0.8	(0.9639, 0.0500)	(0.9793, 0.0682)	(0.9804, 0.0803)	(0.9815, 0.0960)	(0.9828, 0.1164)
			(1.0472, 0.0500)	(1.0228, 0.0674)	(1.0208, 0.0768)	(1.0189, 0.0891)	(1.0174, 0.1082)
0.01	0.20	−0.8	(0.9553, 0.0500)	(0.9764, 0.0505)	(0.9779, 0.0568)	(0.9788, 0.0671)	(0.9803, 0.0793)
			(1.0974, 0.0500)	(1.0331, 0.0510)	(1.0287, 0.0556)	(1.0255, 0.0637)	(1.0219, 0.0712)
		−0.4	(0.9560, 0.0501)	(0.9768, 0.0506)	(0.9777, 0.0589)	(0.9788, 0.0687)	(0.9800, 0.0832)
			(1.0956, 0.0500)	(1.0322, 0.0502)	(1.0284, 0.0563)	(1.0246, 0.0617)	(1.0219, 0.0729)
		0.0	(0.9569, 0.0500)	(0.9774, 0.0500)	(0.9780, 0.0593)	(0.9791, 0.0695)	(0.9804, 0.0827)
			(1.0939, 0.0500)	(1.0347, 0.0579)	(1.0278, 0.0559)	(1.0246, 0.0634)	(1.0218, 0.0748)
		0.4	(0.9577, 0.0500)	(0.9772, 0.0520)	(0.9784, 0.0593)	(0.9792, 0.0705)	(0.9803, 0.0858)
			(1.0921, 0.0500)	(1.0319, 0.0523)	(1.0273, 0.0559)	(1.0244, 0.0646)	(1.0213, 0.0744)
		0.8	(0.9585, 0.0500)	(0.9777, 0.0519)	(0.9787, 0.0597)	(0.9794, 0.0720)	(0.9805, 0.0872)
			(1.0904, 0.0500)	(1.0324, 0.0554)	(1.0275, 0.0583)	(1.0240, 0.0649)	(1.0213, 0.0764)
0.20	0.01	−0.8	(0.9289, 0.0500)	(0.9676, 0.0506)	(0.9728, 0.0500)	(0.9756, 0.0556)	(0.9776, 0.0659)
			(1.0735, 0.0500)	(1.0355, 0.0569)	(1.0275, 0.0500)	(1.0248, 0.0559)	(1.0222, 0.0644)
		−0.4	(0.9295, 0.0500)	(0.9684, 0.0500)	(0.9732, 0.0500)	(0.9758, 0.0559)	(0.9780, 0.0656)
			(1.0716, 0.0500)	(1.0319, 0.0501)	(1.0269, 0.0500)	(1.0244, 0.0561)	(1.0221, 0.0657)
		0.0	(0.9303, 0.0500)	(0.9688, 0.0501)	(0.9736, 0.0500)	(0.9761, 0.0564)	(0.9782, 0.0665)
			(1.0698, 0.0500)	(1.0312, 0.0501)	(1.0267, 0.0509)	(1.0241, 0.0571)	(1.0218, 0.0665)
		0.4	(0.9310, 0.0500)	(0.9690, 0.0508)	(0.9737, 0.0509)	(0.9761, 0.0577)	(0.9782, 0.0681)
			(1.0679, 0.0500)	(1.0305, 0.0500)	(1.0259, 0.0502)	(1.0237, 0.0573)	(1.0216, 0.0676)
		0.8	(0.9318, 0.0500)	(0.9698, 0.0500)	(0.9740, 0.0515)	(0.9761, 0.0593)	(0.9783, 0.0695)
			(1.0660, 0.0500)	(1.0298, 0.0500)	(1.0254, 0.0506)	(1.0236, 0.0588)	(1.0217, 0.0701)

RZ chart, for these in-control scenarios. After determining the optimal couples (K^{*-}, λ^{*-}) or (K^{*+}, λ^{*+}), the EWMA-RZ charts are defined. We then calculate the measure $EARL$ to evaluate the performance of these charts.

Figures 1 shows the effect of precision errors (represented by η_X and η_Y) on the charts' performance given that no accuracy errors (i.e. $\theta_X = \theta_Y = 0$) exist. The $EARL$ values are computed for $\eta_X \in \{0, 0.1, 0.2, ..., 1\}$, $\eta_Y \in \{0, 0.1, 0.2, ..., 1\}$ and for fixed values of $n \in \{1, 15\}$, $\gamma_X = \gamma_Y \in \{0.01, 0.2\}$, $m = 1, b = 1$, $\rho_M = 0$, $\rho_0 = \rho_1 = -0.8$ The obtained results show that the precision errors have a negative influence on the efficiency of the proposed charts: The larger the values of η_X and η_Y, the larger the values of $EARL$. For example, given $n = 1, \Omega_D = [0.9, 1)$, $\rho_0 = \rho_1 = -0.8$, $\gamma_X = \gamma_Y = 0.2$, we obtain $EARL = 82.14$ when $\eta_X = \eta_Y = 0.1$ and $EARL = 91.06$ when $\eta_X = \eta_Y = 0.9$. In this case, when the precision errors are small, say $\eta_X \leqslant 0.5$ and $\eta_Y \leqslant 0.5$, this influence is not significant. For instance, with $n = 1$, $\Omega_I = (1, 1.1]$, $\rho_0 = -0.4, \rho_1 = -0.8$, $\gamma_X = \gamma_Y = 0.01$, we have $EARL = 3.83$ when $\eta_X = \eta_Y = 0.5$ compared to $EARL = 3.57$ when $\eta_X = \eta_Y = 0.0$, i.e. without precision error.

The effect of accuracy errors (represented by θ_X and θ_Y) on the $EARL$ values of the EWMA-RZ control chart, given that no precision errors (i.e. $\eta_X = \eta_Y = 0$) exist, is presented in Figure 2. The calculation is made for the values of $\theta_X \in \{0, 0.005, 0.01, ..., 0.05\}$, $\theta_Y \in \{0, 0.005, 0.01, ..., 0.05\}$ and for fixed values of $n \in \{1, 15\}$, $\gamma_X = \gamma_Y \in \{0.01, 0.2\}$, $m = 1, b = 1$, $\rho_M = 0$, $\rho_0 = \rho_1 = -0.8$ (Figure 1) and $\rho_0 = -0.4, \rho_1 = -0.8$ (Figure 9 in the Appendix). In general, when θ_X increases and θ_Y decreases, $EARL$ increases. For example, given $n = 1, \Omega_I = (1, 1.1]$, $\rho_0 = \rho_1 = -0.8$, $\gamma_X = \gamma_Y = 0.2$, we obtain $EARL = 107.68$ when $\theta_X = 0.005, \theta_Y = 0.05$ and $EARL = 112.25$ when $\theta_X = 0.05, \theta_Y = 0.05$ (Figure 2). However, the change of $EARL$ corresponding to the variation of θ_X and θ_Y when these values are not too large, say $\theta_X, \theta_Y \leqslant 0.025$, is trivial and the value of $EARL$ in these cases is almost equal to the one without accuracy errors. For example, when $n = 1$, $\Omega_D = [0.9, 1)$, $\rho_0 = -0.4, \rho_1 = -0.8$, $\gamma_X = \gamma_Y = 0.01$, we have $EARL = 3.48$ for both cases: $\theta_X = \theta_Y = 0$ and $\theta_X = \theta_Y = 0.025$.

We illustrate the values of $EARL$ corresponding to the change of $\rho_M \in$

Figure 1: The effect of η_X and η_Y on the overall performance of the EWMA-RZ control chart in the presence of measurement errors for $\theta_X = \theta_Y = 0$, $\rho_M = 0$, $m = 1, b = 1$, $n \in \{1, 15\}$, $\gamma_X = \gamma_Y \in \{0.01, 0.2\}$, and $\rho_0 = \rho_1$.

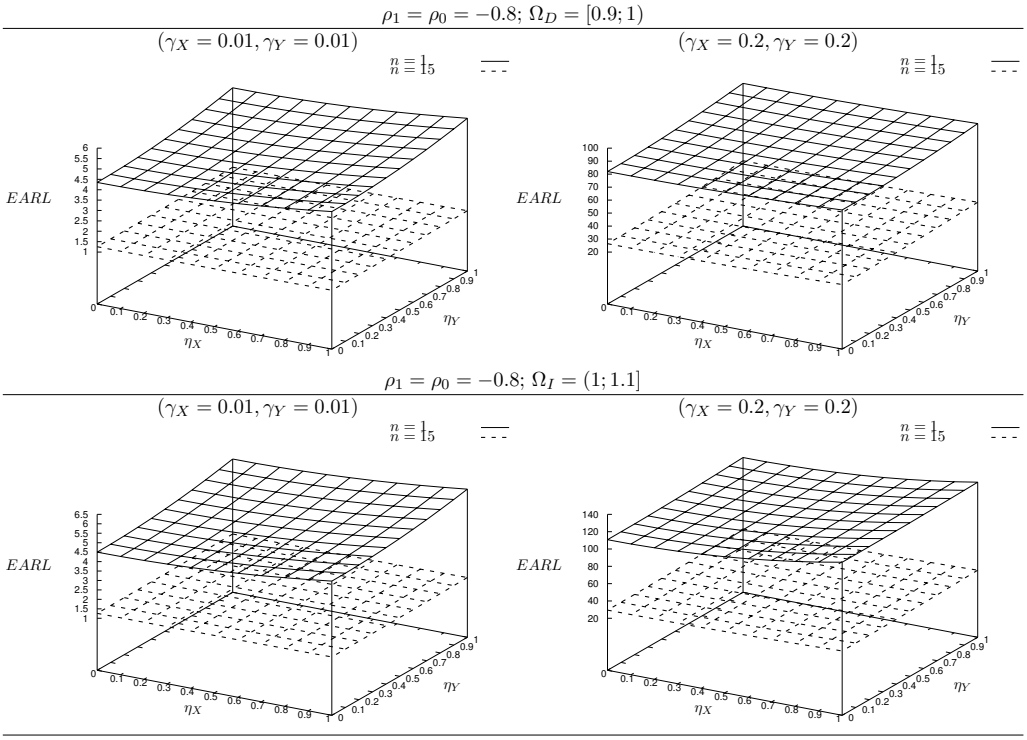

Figure 2: The effect of θ_X and θ_Y on the overall performance of the EWMA-RZ control chart in the presence of measurement errors for $\eta_X = \eta_Y = 0$, $\rho_M = 0$, $m = 1, b = 1$, $n \in \{1, 15\}$, $\gamma_X = \gamma_Y \in \{0.01, 0.2\}$, and $\rho_0 = \rho_1$.

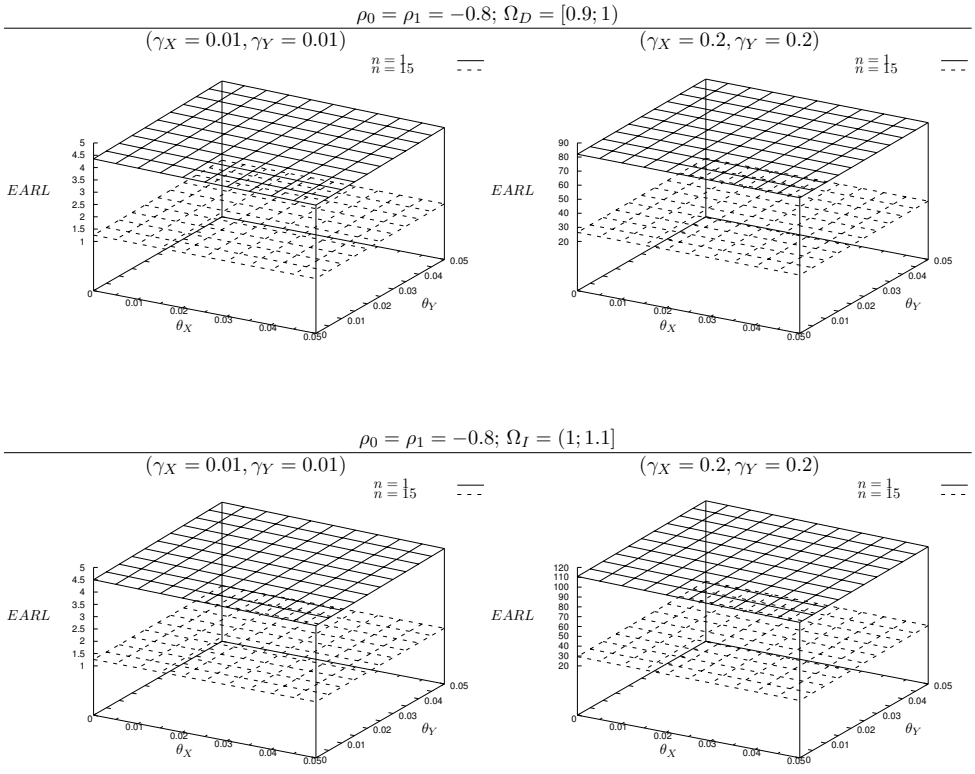

$\{-1, -0.9, \ldots, 0.9, 1\}$ in Figure 3 (for $\rho_0 = \rho_1 = -0.8$) and Figure 10 in the Appendix (for $\rho_0 = -0.4, \rho_1 = -0.8$), given the other values of $n \in \{1, 15\}$, $m = 1, b = 1$, $\gamma_X = \gamma_Y \in \{0.01, 0.2\}$, and the presence of precision errors and accuracy errors, i.e. $\theta_X = \theta_Y = 0.05$, $\eta_X = \eta_Y = 0.28$. The oblique lines in Figures 3-10 show that the increase of ρ_M lead to the decrease of $EARL$. Take the case $n = 1$, $\Omega_D = [0.9, 1)$, $\rho_0 = \rho_1 = -0.8$, $\gamma_X = \gamma_Y = 0.2$ as an example: we have $EARL = 57.75$ when $\rho_M = -0.8$ and $EARL = 51.34$ when $\rho_M = 0.8$ (Figure 10).

A traditional method to reduce the effect of measurement errors in practice is to take multiple measurement per item, which is represented by the value of m. We demonstrate the performance of the EWMA-RZ control charts when m increases from 1 to 10 given the values of $n \in \{1, 15\}$, $\rho_M = 0.4$,$b = 1$, $\gamma_X = \gamma_Y \in \{0.01, 0.2\}$, $\theta_X = \theta_Y = 0.05$, and $\eta_X = \eta_Y = 0.28$ in Figure 4. The obtained results show that for the EWMA-RZ control charts, the increase of m does not improve significantly the chart performance. This is shown by the almost constant lines in these figures. For example, with $n = 1$, $b = 1$, $\gamma_X = \gamma_Y = 0.2$, $\theta_X = \theta_Y = 0.05$, $\eta_X = \eta_Y = 0.28$ and $\rho_0 = \rho_1 = -0.8$ in Figure 4, we obtain an insignificant decrease from $EARL = 82.93$ when $m = 1$ to $EARL = 82.30$ when $m = 10$. Thus, we can conclude that taking multiple measurement is not an effective way to reduce the negative influence of measurement errors on the EWMA-RZ control charts. This finding is in accordance with the one in previous studies of the control chart monitoring RZ considering ME (for example, Nguyen & Tran [13]). From this point of view, we propose that the quality practitioner should improve the measurement system (to reduce the values of η_X, η_Y, for example) rather than spending time for taking multiple measurement per item.

We also consider the influence of b on the performance of the proposed control charts. This influence is shown in Figure 5 for some situations of other parameters, which are $n \in \{1, 15\}$, $\rho_M = 0.4$,$m = 1$, $\gamma_X = \gamma_Y \in \{0.01, 0.2\}$, $\theta_X = \theta_Y = 0.05$, and $\eta_X = \eta_Y = 0.28$. As can be seen from these figures that increasing the values of b can alleviate the negative effects of measurement errors to some degrees. In particular, when b increases from 0.8 to 1.2, the value of $EARL$ decreases. For instance, with $n = 1$, $m = 1$, $\gamma_X = \gamma_Y = 0.2$, $\theta_X = \theta_Y =$

Figure 3: The effect of ρ_M on the overall performance of the EWMA-RZ control chart in the presence of measurement errors for $n = 1$ (-□-) and $n = 15$ (-■-), $m = 1, b = 1$, $\eta_X = \eta_Y = 0.28$, $\theta_X = \theta_Y = 0.05$, $n \in \{1, 15\}$, $\gamma_X = \gamma_Y \in \{0.01, 0.2\}$ and $\rho_0 = \rho_1 = -0.8$.

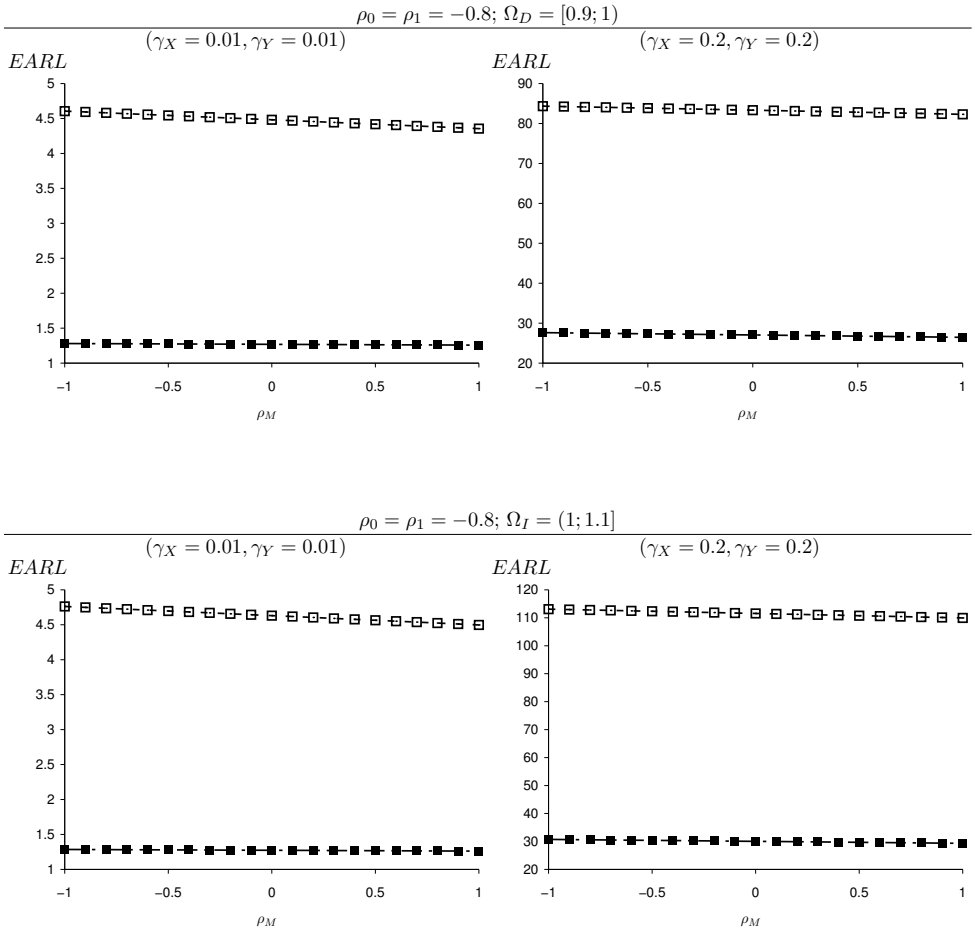

Figure 4: The effect of m on the overall performance of the EWMA-RZ control chart in the presence of measurement errors for $n = 1$ (-□-) and $n = 15$ (-■-), $\eta_X = \eta_Y = 0.28$, $\theta_X = \theta_Y = 0.05$, $n \in \{1, 15\}$, $\rho_M = 0.4$, $b = 1$, $\gamma_X = \gamma_Y \in \{0.01, 0.2\}$ and $\rho_0 = \rho_1 = -0.8$.

$\rho_0 = \rho_1 = -0.8$; $\Omega_D = [0.9; 1)$

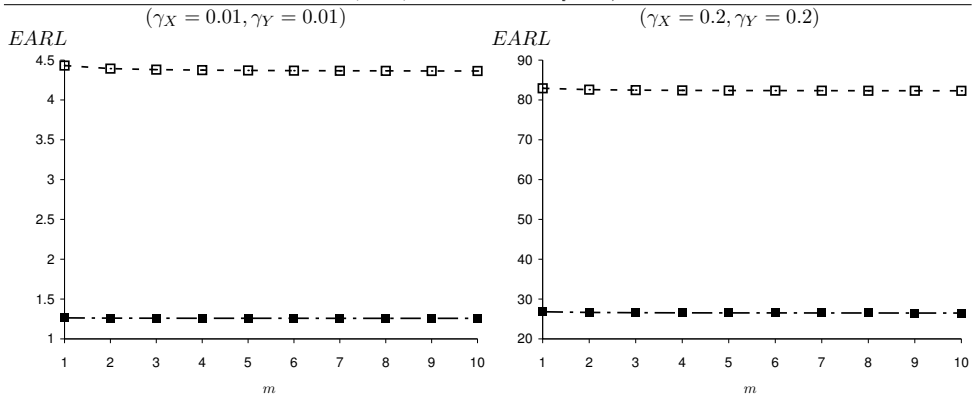

$\rho_0 = \rho_1 = -0.8$; $\Omega_I = (1; 1.1]$

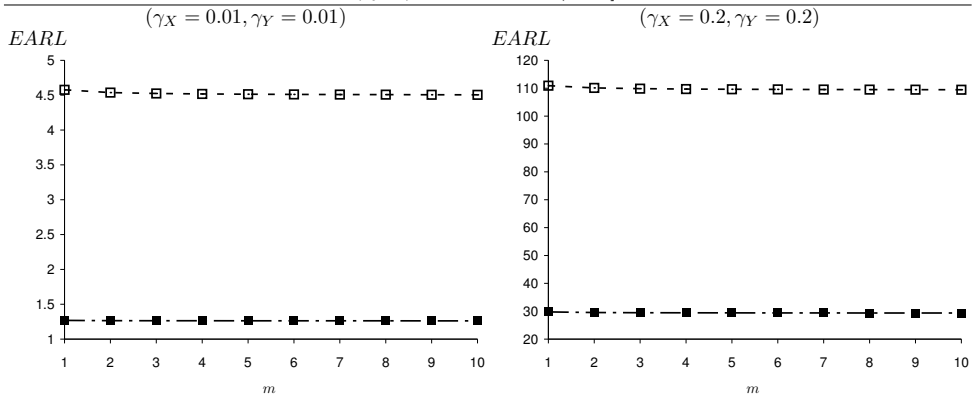

0.05, $\eta_X = \eta_Y = 0.28$ and $\rho_0 = \rho_1 = -0.8$ in Figure 5, we have $EARL = 114.99$ when $b = 0.8$ and $EARL = 114.2$ when $b = 1.2$. Although the increase of b leads to the decrease of the $EARL$, one shoud not consider increasing b as a way to reduce the impact of measurement errors since it will affect the quality of measurement system. The range of b in this study is motivated based on the discussion in Nguyen et al. [14].

Finally, we would like to compare the performance (under the presence of measurement errors) of our proposed charts with the performance of the one-sided Shewhart-RZ control chart investigated in Nguyen & Tran [13]. The obtained result shows that the $EARL$ values corresponding to the one-sided EWMAR-RZ control charts are significantly smaller than the ones corresponding to the one-sided Shewhart-RZ control charts. For example, given $n = 1$, $m = 1$, $\gamma_X = \gamma_Y = 0.2$, $\rho_0 = \rho_1 = -0.8$, $\Omega_D = [0.9, 1)$, $\eta_X = \eta_Y = 0.28$, $\theta_X = \theta_Y = 0.05$, $m = 1$, $\rho_M = 0.4$ we have $EARL = 82.13$ for the EWMA-RZ$^-$ chart (Figure 4 in this study), while $EARL = 110.57$ for the Shewhart-RZ$^-$ chart (Figure 8 in Nguyen & Tran [13]. That is to say, in general, the one-sided EWMA-RZ control charts outperform substantially the one-sided Shewhart-RZ control charts in detecting process shifts regardless of the measurement errors. We also consider the case $\rho_0 \neq \rho_1$, where the results are presented in the Appendix.

6. Illustrative example

In this section, we illustrate an example of the implementation of the EWMA-RZ control charts in the presence of measurement errors. A real context of managing waste batteries in Italy, which was introduced in Tran et al. [22], is considered.

According to the discussion in Tran et al. [22], batteries for recycling are received by collecting facilities incoming disposed material into designated drums, sacks or boxes, denoted as "batches". In practice, these batches usually contain several disposed materials that are not recyclable batteries like small electronic devices, metals, and other kinds of waste. These disposed of materials are a recycling process cost since they should be removed from the batches. In a recycling plant, the process is at the test run stage and the ratio z of recyclable

Figure 5: The effect of b on the overall performance of the EWMA-RZ control chart in the presence of measurement errors for $n = 1$ (-□-) and $n = 15$ (-■-), $\eta_X = \eta_Y = 0.28$, $\theta_X = \theta_Y = 0.05$, $n \in \{1, 15\}$, $\rho_M = 0.4$, $m = 1$, $\gamma_X = \gamma_Y \in \{0.01, 0.2\}$ and $\rho_0 = \rho_1 = -0.8$.

$\rho_0 = \rho_1 = -0.8$; $\Omega_D = [0.9; 1)$

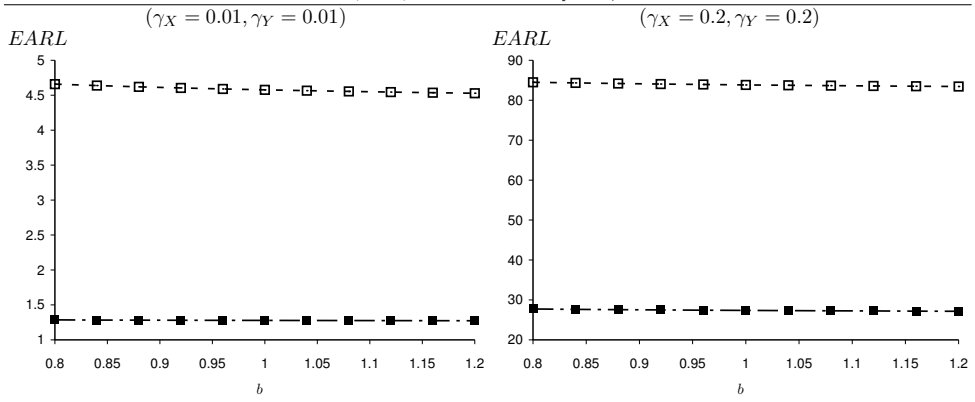

$\rho_0 = \rho_1 = -0.8$; $\Omega_I = (1; 1.1]$

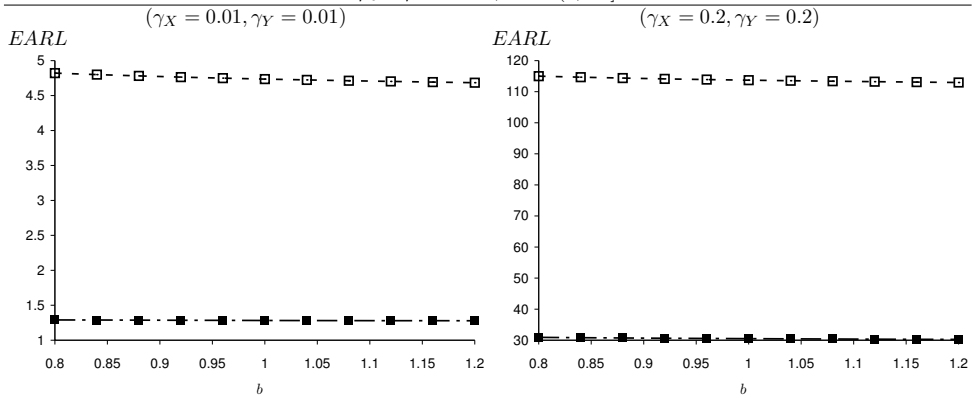

batteries weight (denoted by X) to total batch weight (denoted by Y) is monitored to quantify the cost because of the presence of not recyclable batteries. Suppose that a value of 0.95 is the target of interest for the in-control ratio z_0 to avoid an economic loss.

In the process of monitoring the ratio z, a sample of $n = 5$ is collected at regular intervals $i = 1, 2, \ldots$ with batches having nominal weight 100kg. Due to the variability, the batch weight is considered as a random normal variable $Y \sim N(100, 1)$. Similarly, the recyclable batteries' weight within each batch is a normal random variable with a target mean of $\mu_X = 95$kg. The sample average weights $\bar{X}_i^* = \frac{1}{n}\sum_{j=1}^{n} X_{i,j}^*$ and $\bar{Y}_i^* = \frac{1}{n}\sum_{j=1}^{n} Y_{i,j}^*$ are recorded. Table 2 presents a set of simulated samples of incoming material in the battery recycling process introduced in Tran et al. [22]. In these samples, a decreasing shift has been simulated from sample #11 with the size up to 1% of the in-control ratio z_0. In addition, the coefficients of variations of two variables are $\gamma_X = 0.01$ and $\gamma_Y = 0.01$, and the in-control correlation coefficient between them is $\rho_0 = 0.8$. Similar to Tran et al. [22], we suppose the following parameters of the linear covariate error model: $\theta_X = \theta_Y = 0$, $\eta_X = \eta_Y = 0.28$, $\rho_1 = 0.8, b = 1$, and $\rho_M = 0$. Moreover, we suppose a smoothing $\lambda = 0.2$. Then, the control limit of the EWMA-RZ$^-$ control chart with measurement errors is $LCL^- = 0.9473618$.

Figure 6 illustrates the EWMA-RZ$^-$ control chart. The chart detects the out-of-control samples by plotting them below the control limit, which are the samples #11, #12, #13, and #15. The Shewhart-RZ$^-$ control chart could only detect the abnormality for the sample #11.

7. Concluding remarks

In this paper, we have investigated the effect of measurement errors on the performance of the EWMA-RZ control chart. The assumption of the identity matrix in the linear covariate error model has been extended to the diagonal matrix. This helps to see the impact of this parameter on the proposed charts' performance. Some important conclusions can be drawn from this study as follows.

- Both the precision error and the accuracy error have negative impacts on the one-sided EWMA-RZ control charts. However, when these errors are

Table 2: The battery recycling industry example data

Sample	$X^*_{i,j}$ [kg] / $Y^*_{i,j}$ [kg]					$\bar{X}^*_i$ [kg] / $\bar{Y}^*_i$ [kg]	$\hat{Z}^*_i = \frac{\bar{X}^*_i}{\bar{Y}^*_i}$	Y^{*-}_i
1	95.864	94.731	94.643	94.193	94.328	94.752	0.951	0.9502
	100.891	100.143	100.340	97.740	99.295	99.682		
2	94.969	94.935	94.270	94.663	93.961	94.560	0.956	0.9500
	98.903	96.883	97.329	101.021	100.278	98.883		
3	93.274	95.927	94.961	96.021	95.429	95.122	0.945	0.9490
	101.525	100.461	100.826	98.936	101.398	100.629		
4	95.350	96.128	96.610	95.022	95.737	95.769	0.955	0.9500
	101.137	101.127	100.052	98.796	100.115	100.245		
5	94.697	96.827	94.392	94.197	96.205	95.264	0.955	0.9500
	98.996	100.356	99.860	100.082	99.377	99.734		
6	94.623	93.930	96.532	94.197	93.573	94.571	0.953	0.9500
	99.309	99.727	98.908	98.534	99.745	99.245		
7	94.419	95.445	94.328	95.120	95.880	95.038	0.946	0.9492
	99.936	99.836	101.138	99.668	101.850	100.486		
8	96.144	94.121	96.163	93.803	94.900	95.026	0.953	0.9499
	98.212	100.667	99.683	99.044	101.184	99.758		
9	94.151	94.786	95.127	94.098	94.307	94.494	0.948	0.9495
	99.173	100.873	100.487	100.635	98.675	99.969		
10	96.006	96.319	94.026	94.660	93.948	94.992	0.949	0.9494
	99.392	98.783	100.008	101.235	101.325	100.149		
11	93.436	94.988	93.583	94.831	92.875	93.9426	0.934	**0.9463**
	100.491	100.976	100.815	100.102	100.685	100.614		
12	95.832	95.250	94.402	95.221	95.698	95.281	0.947	**0.9464**
	100.007	101.654	100.648	101.531	99.040	100.576		
13	95.746	93.764	92.958	94.811	94.250	94.306	0.943	0.9457
	99.164	100.864	100.174	99.642	100.309	100.031		
14	95.897	95.408	95.121	94.810	96.402	95.528	0.956	**0.9478**
	101.025	98.955	100.267	99.332	100.238	99.963		
15	95.481	95.595	94.547	95.299	94.600	95.104	0.944	**0.9470**
	99.933	99.406	102.736	100.533	101.300	100.782		

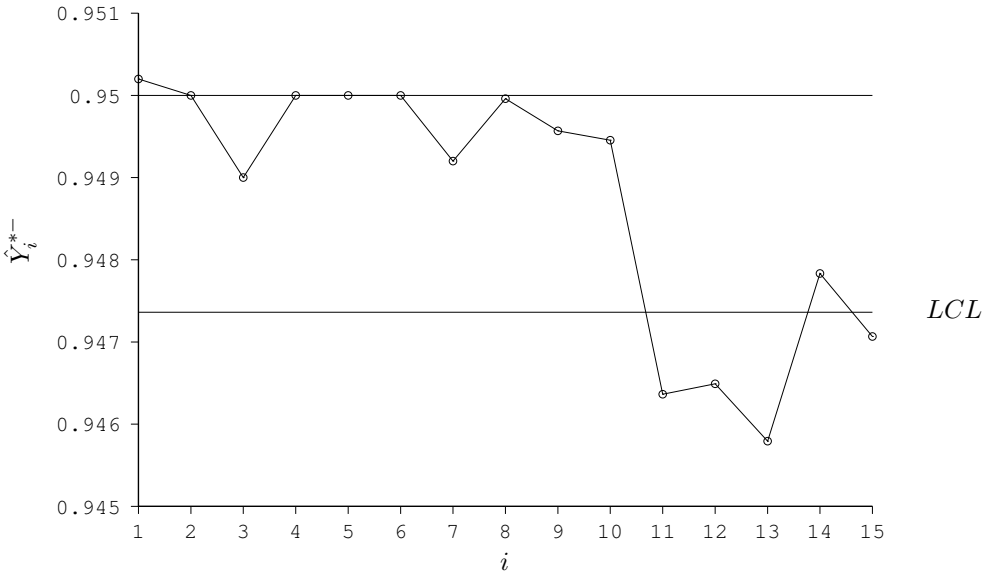

Figure 6: The EWMA-RZ$^-$ control chart in the presence of measurement errors for the battery recycling industry dataset

not too large, say $\eta_X, \eta_Y \leqslant 0.5$ and $\theta_X, \theta_Y \leqslant 0.025$ in this study, these impacts is insignificant.

- Taking multiple measurement per item is not an effective way to reduce the effect of measurement errors on the proposed chart performance.
- Regardless of the measurement errors, the one-sided EWMA-RZ control charts outperform significantly the one-sided Shewhart-RZ control chart in detecting the process shifts.

Future research could be to investigate the effect of measurement error on the control charts monitoring the ratio of random normal variables like the adaptive exponentially weighted moving average-type control chart (Mitra et al. [12]), considering the case of short runs as in Nikolaidis & Tagaras [15] or considering Phase I implementation.

Acknowledgment: The authors thank the anonymous referees for their insightful and valuable suggestions which helped to improve the quality of the final manuscript. This work has been completed while the second authors is visiting the department of Industrial Systems Engineering and Production Design

at Ghent University (UGent). The department's support is highly appreciated.

References

[1] Bersimis, S., Koutras, M. V., & Maravelakis, P. E. (2014). A compound control chart for monitoring and controlling high quality processes. *European Journal of Operational Research*, *233*, 595–603.

[2] Brook, D., & Evans, D. (1972). An approach to the probability distribution of CUSUM run length. *Biometrika*, *59*, 539–549.

[3] Castagliola, P., Celano, G., & Psarakis, S. (2011). Monitoring the coefficient of variation using EWMA charts. *Journal of Quality Technology*, *43*, 249–265.

[4] Celano, G., & Castagliola, P. (2016). Design of a phase II control chart for monitoring the ratio of two normal variables. *Quality and Reliability Engineering International*, *32*, 291–308.

[5] Celano, G., Castagliola, P., Faraz, A., & Fichera, S. (2014). Statistical performance of a control chart for individual observations monitoring the ratio of two normal variables. *Quality and Reliability Engineering International*, *30*, 1361–1377.

[6] Celano, G., Castagliola, P., Fichera, S., & Nenes, G. (2013). Performance of t control charts in short runs with unknown shift sizes. *Computers & Industrial Engineering*, *64*, 56–68.

[7] Daryabari, S. A., Malmir, B., & Amiri, A. (2019). Monitoring bernoulli processes considering measurement errors and learning effect. *Quality and Reliability Engineering International*, *35*, 1129–1143.

[8] Hassani, Z., Amiri, A., & Castagliola, P. (2019). Variable sample size EWMA chart with measurement errors. *Scientia Iranica*, .

[9] Khurshid, A., & Chakraborty, A. B. (2020). Power of control chart for the ratio of two poisson distributions under misclassification error. *Yugoslav Journal of Operations Research*, *430(2)*, 199–208.

[10] Linna, K. W., Woodall, W. H., & Busby, K. L. (2001). The performance of multivariate control charts in the presence of measurement error. *Journal of Quality Technology*, *33*, 349–355.

[11] Marcondes, D. F., & Valk, M. (2020). Dynamic VAR model-based control charts for batch process monitoring. *European Journal of Operational Research*, .

[12] Mitra, A., Lee, K. B., & Chakraborti, S. (2019). An adaptive exponentially weighted moving average-type control chart to monitor the process mean. *European Journal of Operational Research*, *279*, 902–911.

[13] Nguyen, H. D., & Tran, K. P. (2020). Effect of the measurement errors on two one-sided shewhart control charts for monitoring the ratio of two normal variables. *Quality and Reliability Engineering International*, .

[14] Nguyen, H. D., Tran, K. P., Celano, G., Maravelakis, P. E., & Castagliola, P. (2020). On the effect of the measurement error on shewhart t and ewma t control charts. *The International Journal of Advanced Manufacturing Technology*, (pp. 1–16).

[15] Nikolaidis, Y., & Tagaras, G. (2017). New indices for the evaluation of the statistical properties of bayesian $\bar{X}$ control charts for short runs. *European Journal of Operational Research*, *259*, 280–292.

[16] Sabahno, H., Amiri, A., & Castagliola, P. (2018). Performance of the variable parameters t control chart in presence of measurement errors. *Journal of Testing and Evaluation*, *47*, 480–497.

[17] Sabahno, H., Castagliola, P., & Amiri, A. (2020). A variable parameters multivariate control chart for simultaneous monitoring of the process mean and variability with measurement errors. *Quality and Reliability Engineering International*, *36*, 1161–1196.

[18] Song, Z., Mukherjee, A., Liu, Y., & Zhang, J. (2019). Optimizing joint location-scale monitoring–an adaptive distribution-free approach with minimal loss of information. *European Journal of Operational Research*, *274*, 1019–1036.

[19] Song, Z., Mukherjee, A., & Zhang, J. (2021). Some robust approaches based on copula for monitoring bivariate processes and component-wise assessment. *European Journal of Operational Research*, *289*, 177–196.

[20] Teoh, W. L., Khoo, M. B., Castagliola, P., Yeong, W. C., & Teh, S. Y. (2017). Run-sum control charts for monitoring the coefficient of variation. *European Journal of Operational Research*, *257*, 144–158.

[21] Tran, K. P., Castagliola, P., & Celano, G. (2016). Monitoring the ratio of two normal variables using EWMA type control charts. *Quality and Reliability Engineering International*, *32*, 1853–1869.

[22] Tran, K. P., Castagliola, P., & Celano, G. (2016). The performance of the Shewhart-RZ control chart in the presence of measurement error. *International Journal of Production Research*, *54*, 7504–7522.

Appendix

A brief review of the distribution of the sample of the ratio

Let $\mathbf{W} = (X, Y)^T$ be a bivariate normal random vector with the mean vector $\boldsymbol{\mu_W}$ and the variance-covariance matrix $\boldsymbol{\Sigma_W}$ where

$$\boldsymbol{\mu_W} = \begin{pmatrix} \mu_X \\ \mu_Y \end{pmatrix}, \quad \boldsymbol{\Sigma_W} = \begin{pmatrix} \sigma_X^2 & \rho\sigma_X\sigma_Y \\ \rho\sigma_X\sigma_Y & \sigma_Y^2 \end{pmatrix}, \tag{29}$$

in which ρ is the correlation coefficient between X and Y. By definition, the coefficients of variation of the two random variables X and Y, and their standard-deviation ratio are $\gamma_X = \frac{\sigma_X}{\mu_X}$ $\gamma_Y = \frac{\sigma_Y}{\mu_Y}$, and $\omega = \frac{\sigma_X}{\sigma_Y}$ respectively.

The ratio of X to Y is defined as $Z = X/Y$. In the literature, the distribution of Z is a major concern in several studies. As discussed in Tran et al. [22], when the coefficient of variation of X and Y takes small values, for example, within the range $[0, 0.2]$, the distribution of Z can be well approximated by the following formula, which is proposed by Celano & Castagliola [4]:

$$F_Z(z|\gamma_X, \gamma_Y, \omega, \rho) \simeq \Phi\left(\frac{A}{B}\right), \tag{30}$$

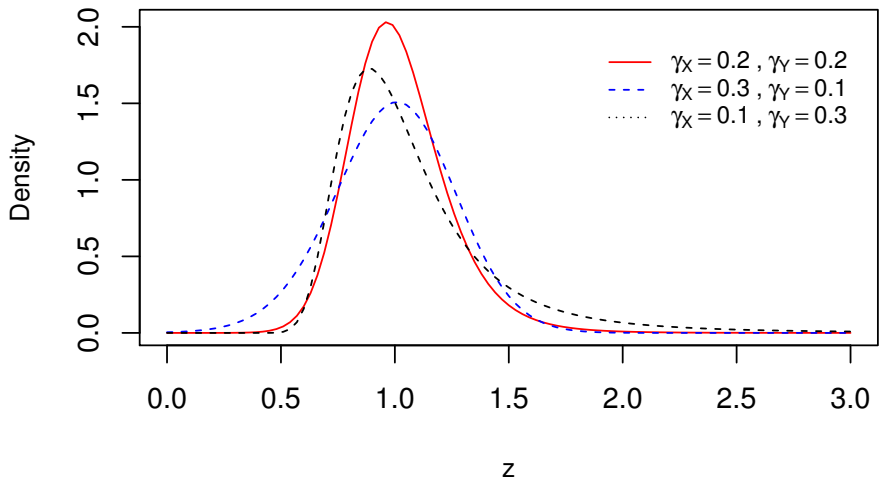

Figure 7: The probability density function of Z for the case $\rho = 0.5$, $\omega = \gamma_X/\gamma_Y$ and different values of γ_X, γ_Y.

where $\Phi(.)$ is the $c.d.f$ (cumulative distribution function) of the standard normal distribution, and where A and B are functions of z, γ_X, γ_Y, ω and ρ in which

$$\begin{aligned} A &= \frac{z}{\gamma_Y} - \frac{\omega}{\gamma_X}, \\ B &= \sqrt{\omega^2 - 2\rho\omega z + z^2}. \end{aligned}$$

The authors (Celano & Castagliola [4]) also showed that the $p.d.f$ (probability density function) of Z can be approximated by

$$f_Z(z|\gamma_X, \gamma_Y, \omega, \rho) \simeq \left(\frac{1}{B\gamma_Y} - \frac{(z-\rho\omega)A}{B^3}\right) \times \phi\left(\frac{A}{B}\right), \tag{31}$$

where $\phi(.)$ is the $p.d.f$ of the standard normal distribution.

Figure 7 illustrates the $p.d.f$ of Z for the case $\rho = 0.5$, $\omega = \gamma_X/\gamma_Y$ and some different values of γ_X and γ_Y.

The Markov chain method to calculate ARL

Suppose that the in-control ratio z_0 is shifted to $z_1 = \tau \times z_0$ due to an out-of-control condition, where $\tau > 0$ is the shift size. In addition, when the process

is shifted, the coefficient of correlation is also shifted from $\rho = \rho_0$ to $\rho = \rho_1$. The sizes $\tau < 1$ correspond to a decrease of the in-control ratio z_0, while the sizes $\tau > 1$ correspond to its increase.

In the Markov chain approach, we devide the control interval into several subintervals, corresponding to severl states of the Markow chain. Let $p+2$ be the states of the chain, where the transient states $0, 1, \ldots, p$ belong to the control interval and the state $p+1$ is a absorbing state: it represents a signal from the chart. Then, we can express the transition probability matrix $\mathbf{P}$ of the Markov chain as

$$\mathbf{P} = \begin{pmatrix} \mathbf{Q} & \mathbf{r} \\ \mathbf{0}^T & 1 \end{pmatrix} = \begin{pmatrix} Q_{0,0} & Q_{0,,1} & \cdots & Q_{0,p} & r_0 \\ Q_{1,0} & Q_{1,1} & \cdots & Q_{1,p} & r_1 \\ \vdots & \vdots & & & \vdots \\ Q_{p,0} & Q_{p,1} & \cdots & Q_{p,p} & r_p \\ 0 & 0 & \cdots & 0 & 1 \end{pmatrix}.$$

where $\mathbf{Q}$ is a $(p+1, p+1)$ matrix of transient probabilities, $\mathbf{0} = (0, 0, \ldots, 0)^T$ and $\mathbf{r}$ is a $(p+1)$ vector satisfying $\mathbf{r} = (\mathbf{1} - \mathbf{Q1})$ (i.e., row probabilities must sum to 1) with $\mathbf{1} = (1, 1, \ldots, 1)^T$.

In particular, the interval control $[z_0, UCL^+]$ (resp.$[LCL^-, z_0]$) of the EWMA-RZ$^+$ (resp. EWMA-RZ$^-$) chart is divided into p subintervals of width 2δ, where $\delta = \frac{K^+ - 1}{2p}$ (resp. $\delta = \frac{1 - K^-}{2p}$). Similar to Tran et al. [21], let H_j denote the midpoint of the jth subinterval, $j = 1, \ldots, p$ and let $H_0 = z_0$ correspond to the "restart state" feature of our charts. Then, the generic elements $Q_{i,j}$, $i = 0, 1, \ldots, p$, of the matrix $\mathbf{Q}$ are calculated by

- for the EWMA-RZ$^+$ chart,

$$Q_{i,0} = F_{\hat{Z}_i^*}\left(\frac{1 - (1 - \lambda^+)H_i}{\lambda^+} \middle| \frac{\gamma_{X^*}}{\sqrt{n}}, \frac{\gamma_{Y^*}}{\sqrt{n}}, \omega^*, \rho^* \right); \tag{32}$$

- for the EWMA-RZ$^-$ chart,

$$Q_{i,0} = 1 - F_{\hat{Z}_i^*}\left(\frac{1 - (1 - \lambda^-)H_i}{\lambda^+} \middle| \frac{\gamma_{X^*}}{\sqrt{n}}, \frac{\gamma_{Y^*}}{\sqrt{n}}, \omega^*, \rho^* \right); \tag{33}$$

- for both charts, when $j = 1, 2, \ldots, p$,

$$\begin{aligned} Q_{i,j} = F_{\hat{Z}_i^*}\left(\frac{H_j + \delta - (1 - \lambda)H_i}{\lambda} \middle| \frac{\gamma_{X^*}}{\sqrt{n}}, \frac{\gamma_{Y^*}}{\sqrt{n}}, \omega^*, \rho^* \right) \\ - F_{\hat{Z}_i^*}\left(\frac{H_j - \delta - (1 - \lambda)H_i}{\lambda} \middle| \frac{\gamma_{X^*}}{\sqrt{n}}, \frac{\gamma_{Y^*}}{\sqrt{n}}, \omega^*, \rho^* \right), \end{aligned} \tag{34}$$

where $F_{\hat{Z}_i^*}(\dots)$ is the *c.d.f* of $\hat{Z}_i^*$ and λ is either λ^+ (EWMA-RZ$^+$ chart) or λ^- (EWMA-RZ$^-$ chart).

After determining the transition probability matrix $\mathbf{Q}$, the ARL is calculated by the following formula (see Tran et al. [21])

$$ARL = \mathbf{q}^T(\mathbf{I} - \mathbf{Q})^{-1}\mathbf{1}, \tag{35}$$

where $\mathbf{q}$ is a $(p+1, 1)$ vector of initial probabilities associated with the $p+1$ transient states, i.e., $\mathbf{q} = (q_0, q_1, \dots, q_p)^T$. Concerning the zero-state condition, the vector $\mathbf{q}$ becomes $\mathbf{q} = (1, 0, \dots, 0)$. When the number p of subintervals is sufficiently large ($p = 200$ in this study), this finite approach provides an effective method to evaluate accurately the run-length properties of the proposed control charts.

The effect of parameters on the overall performance of the EWMA-RZ control chart in presence of measurement errors when $\rho_0 \neq \rho_1$

Figure 8: The effect of η_X and η_Y on the overall performance of the EWMA-RZ control chart in the presence of measurement errors for $\theta_X = \theta_Y = 0$, $\rho_M = 0$, $n \in \{1, 15\}$, $\gamma_X = \gamma_Y \in \{0.01, 0.2\}$, and $\rho_0 \neq \rho_1$.

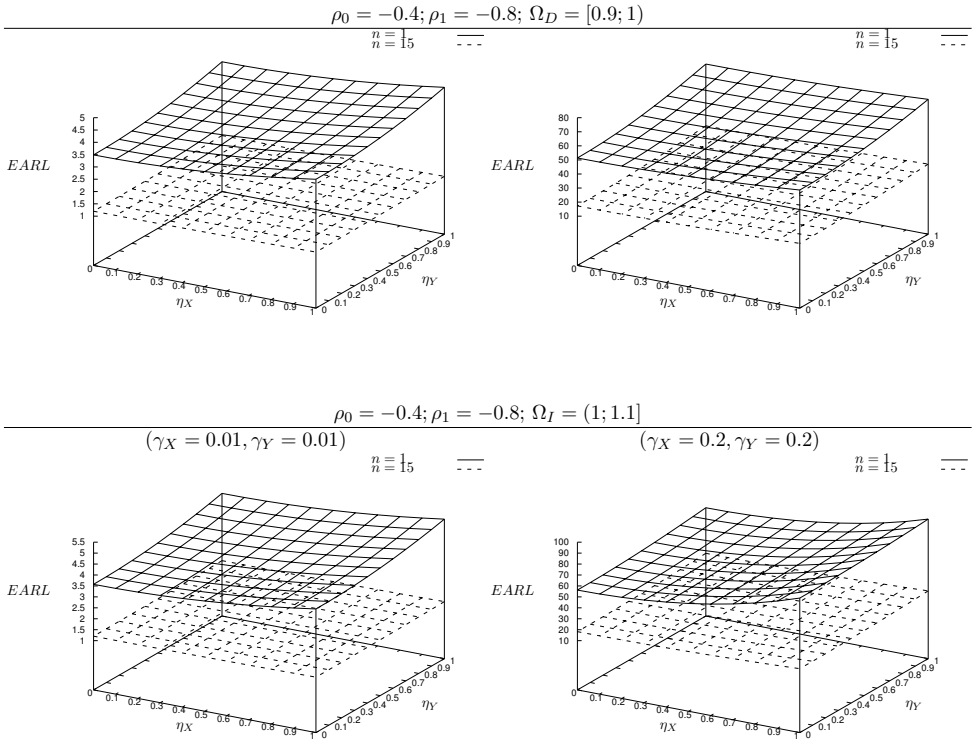

Figure 9: The effect of θ_X and θ_Y on the overall performance of the EWMA-RZ control chart in the presence of measurement errors for $\eta_X = \eta_Y = 0$, $\rho_M = 0$, $n \in \{1, 15\}$, $\gamma_X = \gamma_Y \in \{0.01, 0.2\}$, and $\rho_0 \neq \rho_1$.

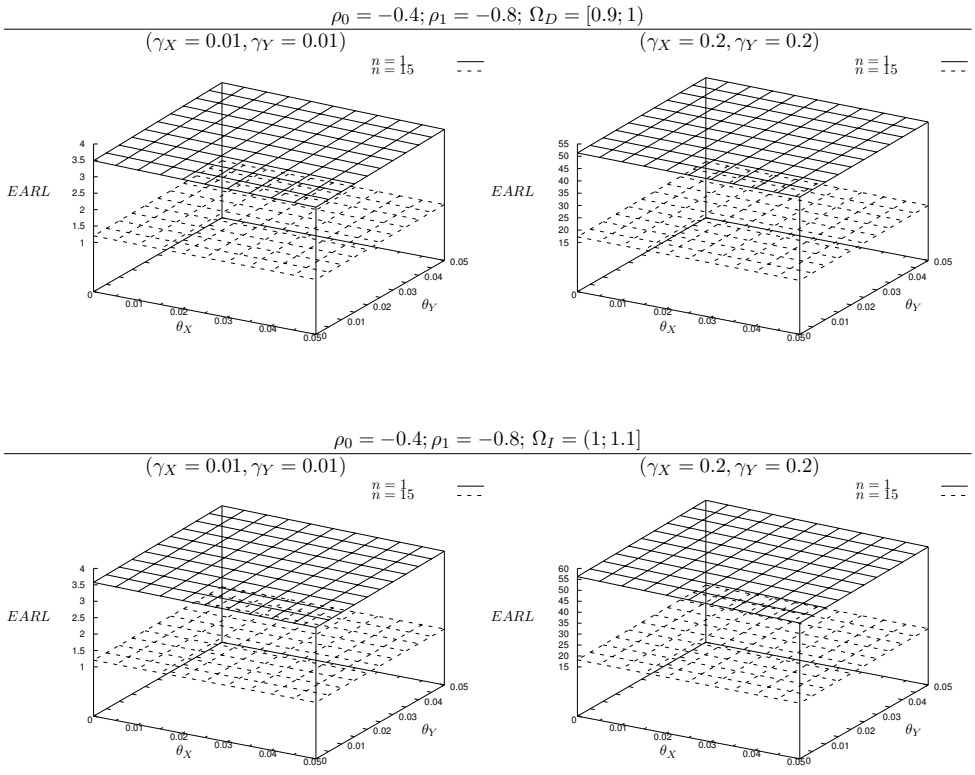

Figure 10: The effect of ρ_M on the overall performance of the EWMA-RZ control chart in the presence of measurement errors for $n = 1$ (-□-) and $n = 15$ (-■-), $m = 1, b = 1$, $\eta_X = \eta_Y = 0.28$, $\theta_X = \theta_Y = 0.05$, $n \in \{1, 15\}$, $\gamma_X = \gamma_Y \in \{0.01, 0.2\}$ and $\rho_0 = -0.4, \rho_1 = -0.8$.

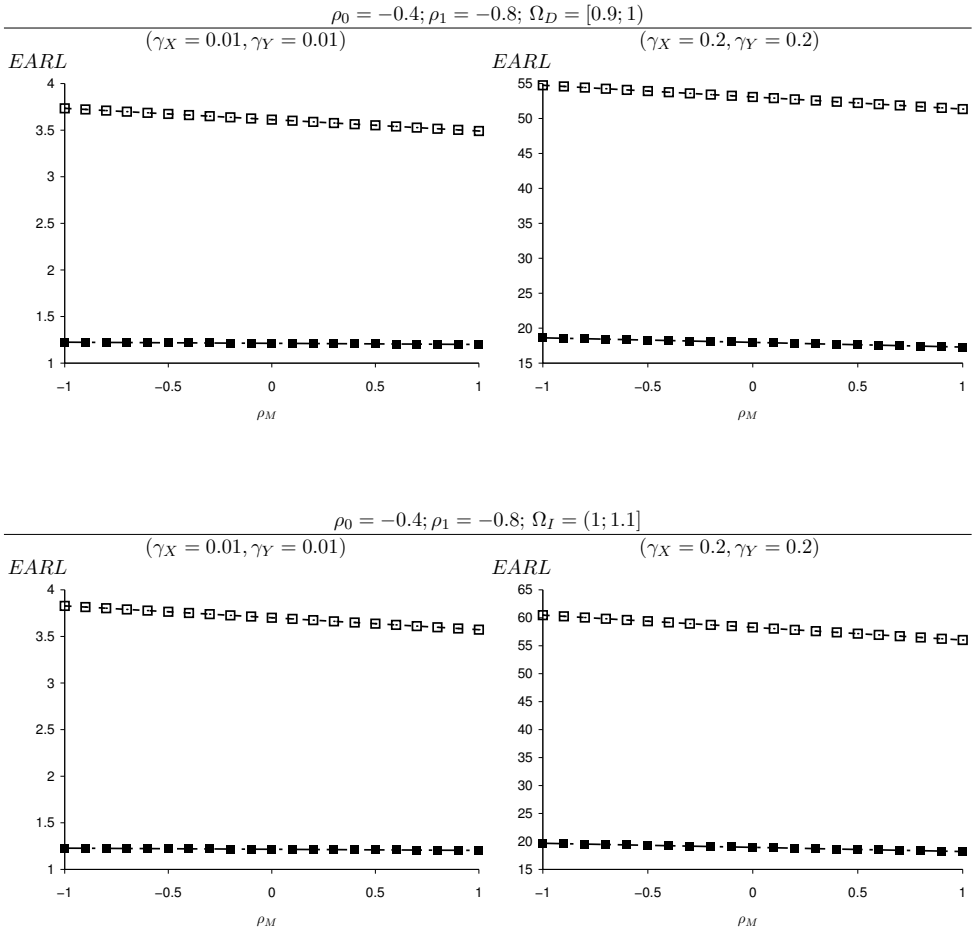

Figure 11: The effect of m on the overall performance of the EWMA-RZ control chart in the presence of measurement errors for $n = 1$ (-□-) and $n = 15$ (-■-), $\eta_X = \eta_Y = 0.28$, $\theta_X = \theta_Y = 0.05$, $n \in \{1, 15\}$, $\rho_M = 0.4$, $b = 1$, $\gamma_X = \gamma_Y \in \{0.01, 0.2\}$ and $\rho_0 = -0.4, \rho_1 = -0.8$.

$\rho_0 = -0.4; \rho_1 = -0.8;\ \Omega_D = [0.9; 1)$

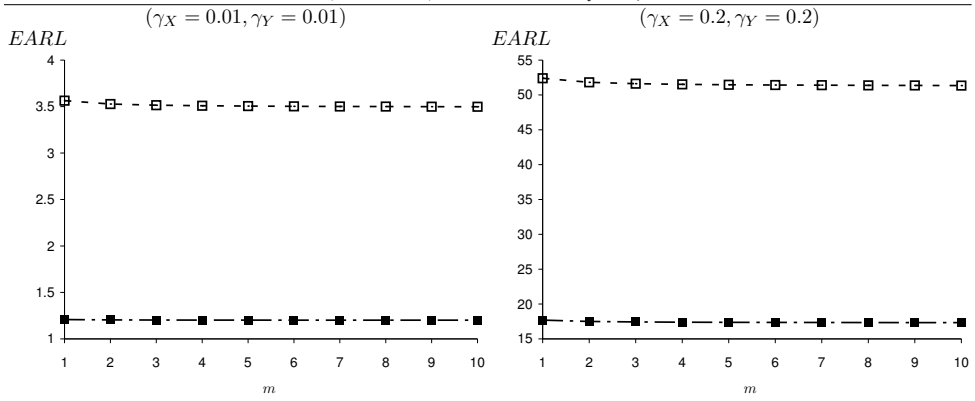

$\rho_0 = -0.4; \rho_1 = -0.8;\ \Omega_I = (1; 1.1]$

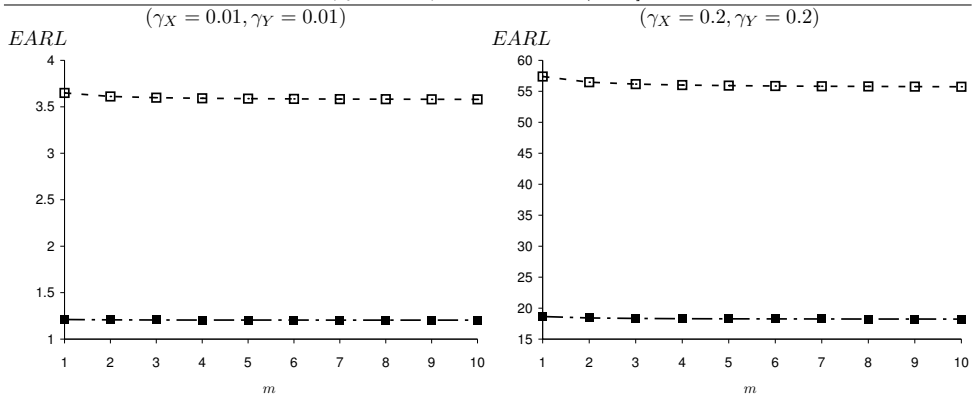

Figure 12: The effect of b on the overall performance of the EWMA-RZ control chart in the presence of measurement errors for $n = 1$ (-□-) and $n = 15$ (-■-), $\eta_X = \eta_Y = 0.28$, $\theta_X = \theta_Y = 0.05$, $n \in \{1, 15\}$, $\rho_M = 0.4$, $m = 1$, $\gamma_X = \gamma_Y \in \{0.01, 0.2\}$ and $\rho_0 = -0.4, \rho_1 = -0.8$.

$\rho_0 = -0.4; \rho_1 = -0.8;\ \Omega_D = [0.9; 1)$

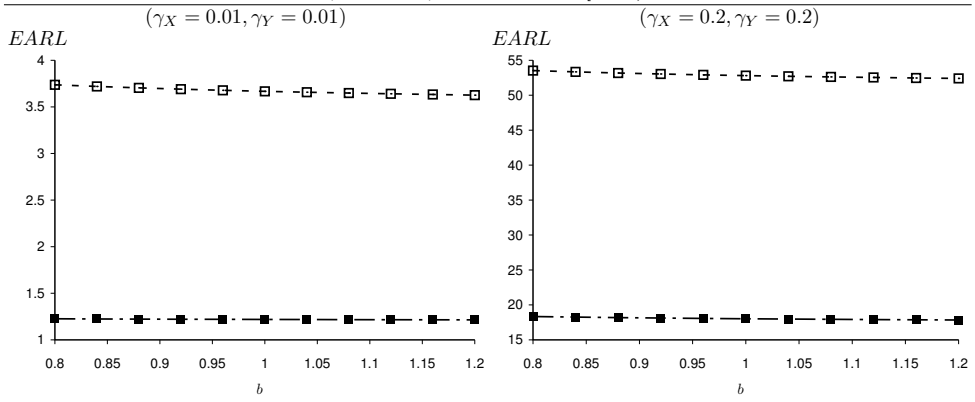

$\rho_0 = -0.4; \rho_1 = -0.8;\ \Omega_I = (1; 1.1]$